NJC

Cite this: *New J. Chem.*, 2012, **36**, 759–767

www.rsc.org/njc

PAPER

Au(I)- and Pt(II)-*N*-heterocyclic carbene complexes with picoline functionalized benzimidazolin-2-ylidene ligands; synthesis, structures, electrochemistry and cytotoxicity studies†

Sirsendu Das Adhikary,[a] Dipayan Bose,[b] Partha Mitra,[c] Krishna Das Saha,[b] Valerio Bertolasi[d] and Joydev Dinda*[a]

Received (in Montpellier, France) 2nd November 2011, Accepted 9th December 2011
DOI: 10.1039/c2nj20928d

Novel Au(I)-*N*-heterocyclic carbene complexes, 1-methyl-3-(2-pyridylmethyl)-benzimidazolylidenegold(I)-chloride, **1**; **1**-benzyl-3-(2-pyridylmethyl)-benzimidazolylidenegold(I)chloride, **2**; and Pt(II)-*N*-heterocyclic carbene complexes 1-methyl-3-(2-pyridylmethyl) benzimidazolylidene platinum(II)chloride, **3**; and 1-benzyl-3-(2-pyridylmethyl) benzimidazolylidene platinum-(II)chloride, **4**, have been synthesized, based on CN-donor proligands 1-alkyl-3-(2-pyridylmeth-yl)-benzimidazoliumchloride **L1** and **L2** [alkyl, R = $-CH_3$ = **L1**; R = $-CH_2Ph$ = **L2**]. All the compounds have been synthesized and characterized by different spectroscopic methods. The Au(I) complexes **1** and **2** have been synthesized by a silver carbene transfer method. The solid-state structures of **1** and **3** have been determined by single crystal X-ray diffraction studies. The square planar Pt(II) complexes **3** and **4** show a reversible Pt(II)/Pt(IV) couple at 0.69 eV and 0.67 eV respectively. Among the complexes **1–4**, complexes **1** and **3** have been used for cytotoxicity studies on the cell lines B16F10 (mouse melanoma), HepG2 (human hepatocarcinoma) and HeLa (human cervical carcinoma). IC_{50} values are compared with cisplatin, among **1** and **3**, the Au(I) complex **1** is more effective than Pt(II) complex **3**.

Introduction

N-Heterocyclic carbenes (NHCs) are defined as singlet carbenes, in which the divalent carbenic center is coupled directly with at least one nitrogen atom within the heterocycle.[1–5] Ofele *et al.* and Wanzlick *et al.* in 1960 first reported the existence of NHCs[6–8] and in 1991 Arduengo and his co-workers first successfully isolated the same.[9] Thereafter, *N*-heterocyclic carbenes (NHCs) have become universally accepted ligands in organometallic and inorganic chemistry.[10,11] Contrarily to other carbenes, which are generally found to be electrophilic, *N*-heterocyclic carbenes are electron-rich nucleophilic scaffolds, in which the carbene center enjoys the benefits from the stabilization related to both the σ-electron-withdrawing and π-electron-donating nature of the nitrogen centers. Due to their strong σ-electron donating properties, they can be treated as alternatives of phosphine.[12–14] Because of their unique electronic dedication, they can bind to a broad range of transition metals, which participate in catalysis.[15–19] On the other hand, fine delicate tuning of physical and electronic properties of NHCs is very possible, which donates different electron density to the metal centers with efficient catalysis.[20–24]

The metal based drugs occupied a considerable room in pharmaceutical chemistry where metal plays an important role.[25–29] After successful isolation of NHC by Arduengo in 1991 it is mainly being used in catalysis; recent studies of NHC complexes as anticancer agents have opened the door to another emerging field.[30–41] Among the other available drugs, newly modified artilleries to fight against cancer are constantly needed and it's a huge challenge to design a suitable drug. Advances in the metal-drug research boosted after discovery of anticancer activity of cisplatin, $PtCl_2(NH_3)_2$.[25] Though cisplatin and related platinum-based drugs have been extensively used as anticancer agents for a long time, they suffered from several drawbacks; some cancer lines are resistant to cisplatin. Other platinum anticancer drugs like platinum(II)-containing oxaliplatin, carboplatin, picoplatin (JM473), nedaplatin (JM118), or redox-active platinum(IV)-based satraplatin, tetraplatin and ormaplatin are used in clinical practice, or in current

[a] *School of Applied Science, "Applied Synthetic Chemical Research Lab.", Haldia Institute of Technology, Haldia-721657, Purba Medinipur, West Bengal, India*
[b] *Department of Biochemistry, Indian Institute of Chemical Biology, Jadavpur, Kolkata-700032, West Bengal, India*
[c] *Department of Inorganic Chemistry, Indian Association for the Cultivation of Sciences, Jadavpur, Kolkata-700032, West Bengal, India*
[d] *Dipartimento di Chimica and Centro di Strutturistica Diffrattometrica, Universita' di Ferrara, Via L. Borsari, 46, Italy*

† CCDC reference numbers 834096 (**1**) and 834097 (**3**). For crystallographic data in CIF or other electronic format see DOI: 10.1039/c2nj20928d

clinical trials.[42] Yet, tremendous efforts are being expended to develop better platinum drug therapies. As metal-NHCs (M-NHCs) are being used as anticancer agents, Pt(II) complex of 1-alkyl-3-(2-pyridylmethyl)benzimidazolylidene would be the right choice because of long antifungal history of benzimidazole and occurrence in bio-organometallic compound vitamin B_{12} *etc.*

The anticancer potential of gold complexes has been recently reviewed.[43] Auranofin, an antirheumatic agent and other gold(I) complexes bearing the linear S-Au-PR_3 moiety were found to be very effective as metallo drugs. The idea of replacing phosphines by NHCs—which are better σ-donor substituents—has emerged and NHC analogues of Auranofin have been synthesized;[44,45] capitalizing the same idea Berners-Price and Barnard obtained excellent results against mouse cancer cells using Au(I)-NHC.[46] Panda and Ghosh have also developed the Au(I)-NHC with excellent efficiency against HeLa cell proliferation.[38] Berners-Price and Filipovska *et al.* made a new approach to mitochondria-targeted antitumor agents in the design of Au(I)-*N*-heterocyclic carbene compounds, where they carry both selective mitochondria targeting and selective thioredoxin reductase inhibition properties within the same single molecule.[47] Being inspired by the recent findings, we became interested to study the anticancer activity of 1-alkyl-3-(2-pyridylmethyl)-benzimidazolylidenegold(I)-chloride.

Result and discussion

Synthetic strategy

The synthesis of 1-methyl/benzyl-3-(2-pyridylmethyl)benzimidazoliumchloride was started from 1-methyl/benzyl-benzimidazole and picolyl chloride hydrochloride in ethanol at basic medium as reported earlier[49,50a] and synthesis and study of other chelating benzimidazolylidene ligands coordinated to transition metals have also been reported.[50b,c] Here, strategically we have introduced the N-donor centre in the 1-methyl/benzyl-3-(2-pyridylmethyl)benzimidazoliumchloride by incorporating the *N*-(2-pyridylmethyl) group to make the system more softer than 1,3-bis[-methyl/benzyl]benzimidazoliumchloride and to mimic with a ppy like system (shown in Chart 1). Au-NHC-Cl complexes **1** and **2** were synthesized from **L1** and **L2** in dichloromethane at room temperature (as shown in Scheme 1) by a silver carbene trans-metallation method.[55–57] Formation of the Au-NHCs from the pro-ligands was confirmed by the absence of imidazolium CH_2 proton at *ca.* 10.56 ppm and down field shift of all aromatic protons. Their ^1H and ^{13}C NMR spectra and CHN data are consistent with the proposed formula. In complex **2**, a 14 ppm shift (154 ppm–168 ppm] of carbenic carbon was observed in $^{13}CNMR$ spectra. The platinum complexes **3** and **4** were also synthesized by using the precursors sodium acetate, K_2PtCl_4 and respective proligands. Formation of **3** and **4** was confirmed by the disappearance of imidazolium CH_2 proton; ^{13}C NMR spectra exhibited singlets at 184.5 and 184.2 ppm for **3** and **4**, respectively, characteristic of the carbenic carbon resonances.[58]

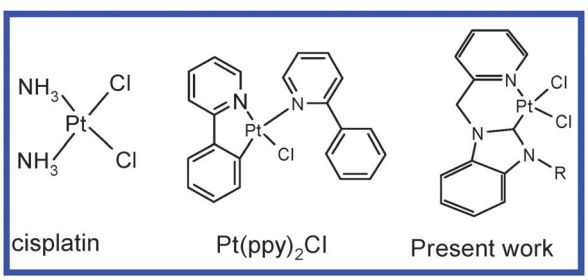

Chart 1

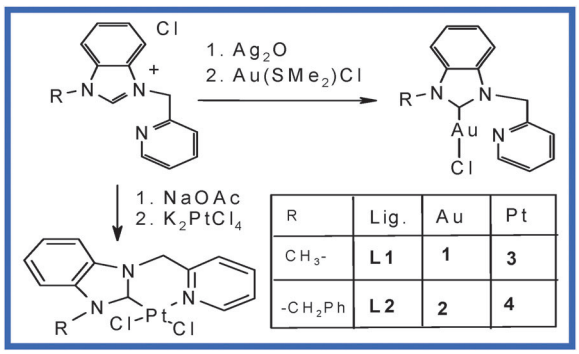

R	Lig.	Au	Pt
CH_3-	L1	1	3
-CH_2Ph	L2	2	4

Scheme 1 Synthesis of Au(I) and Pt(II)–NHC complexes.

Spectroscopic description

The electronic spectra of the complexes **1** and **2** were studied in dichloromethane, the absorbance was observed at 325 and 327 nm, respectively, with two other peaks near 206 and 255 nm, blue shifted in comparison with $Au(ppy)_2^+$ (ppy = phenylpyridine) due to strong σ-donor and weak π-acceptor properties of electron-rich NHC ligands compared to bpy (2,2′-bipyridine) and ppy ligands. Indeed, the NHC ligands have higher electron donating capability than 2,2′-bipyridine or phenylpyridine and the energy level for the π* orbital (LUMO) is higher; therefore the HOMO–LUMO energy gap of **1** and **2** is higher than in analog complexes of a ppy system.[59,60]

The UV-Vis absorption spectra of Pt-NHC complexes were investigated and also compared with those of $Pt(ppy)_2Cl$.[59,60] The absorption spectra of **3** and **4** have intense bands appearing in the ultraviolet region of the spectrum 300–390 nm. The π–π* transition is accompanied by weaker bands extending into the region from 300–320 nm that have been assigned for spin-forbidden transitions. Theoretical studies sometimes are helpful to explain the absorption spectra. Theoretical studies under B3LYP/LANL2DZ of the complex **3** show the HOMO (E_0 = −0.21368 au) to be mainly centered on the platinum and benzimidazole, whereas, the LUMO (E_0 = −0.08670 au) is populated by benzimidazole. Therefore, it is assumed that the charge transfer from HOMO to LUMO is mixed ILCT (interligand charge transfer)/MLCT (metal to ligand charge transfer).[59,60]

X-Ray crystal structural description of Au-complex, 1

The molecular structure of **1** is established by X-ray diffraction studies and depicted in Fig. 1. The crystallographic parameters are listed in Table 1 and selected bond parameters are listed in Table 2.

The gold complex crystallizes in the monoclinic space group '*P*-1'. Its asymmetric unit consists of an independent gold atom, which is bonded together by carbene carbon of 1-methyl-3-(picolyl)benzimidazolydene ligands and a chloride atom.

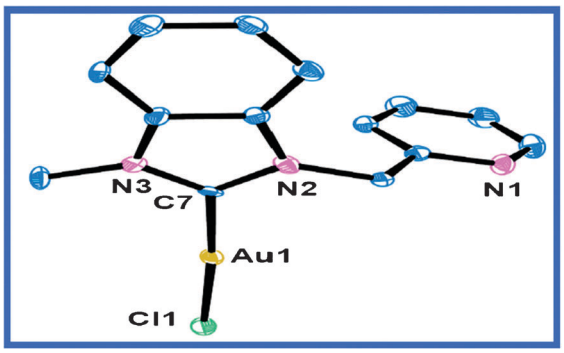

Fig. 1 Single crystal X-ray structure of complex **1** (50% probability, H atoms are removed for clarity).

The $N_{pyridine}$ remains uncoordinated like the earlier Ag-complex.[50] The Au–$C_{carbene}$ and Au–Cl bond distances of 1.999(8) and 2.290(2) Å, respectively, are consistent with those of known Au(I)–NHC complexes having a $C_{carbene}$–Au–Cl motif.[56,57] Mononuclear gold-NHC complexes often show intermolecular gold–gold interactions.[56,57,61,62] The closest intermolecular Au–Au distance is 3.813 Å for **1** and it shows weak aurophilic interaction. The molecules are arranged face to face in *trans* orientations, where Au···Au interaction leads to an infinite chain (shown in Fig. 2). The weak H-bonding through C(12)–H(12)···Cl(1) 2.626(5) Å and C(4)–H(4)···Cl(1) 2.776(9) Å brings two Au(I) closer to each other.

The existence of metal–metal interactions of the coinage metals is widely acknowledged, particularly for gold(I). The structural discussion will remain incomplete if we ignore d^{10}–d^{10} interactions. Gold has been shown to form complexes with particularly strong aurophilic interactions due to relativistic effects.[56,57] The strength of the d^{10}–d^{10} interactions for metal(I)–metal(I) systems is weaker than covalent bonds, but stronger than London dispersion forces. Given this, it is not surprising that aurophilic interactions play a key role in the formation of diverse gold(I)–gold(I) architectures in the solid state, that is really observed in **1**.

Table 2 Selected bond lengths (Å) and bond angles (°) of **1**

Bond lengths (Å)	Bond angles (°)
Au(1)–C(7) = 1.999(8)	C(7)–Au(1)–Cl(1) = 108.5(7)
Au(1)–Cl(1) = 2.290(2)	N(2)–C(7)–N(3) = 176.1(2)
N(2)–C(7) = 1.352(10)	
N(3)–C(7) = 1.332(11)	

Analysis and description of X-ray crystal structure of 3

The solid state structure of **3** is identified by X-ray crystallography, the ORTEP view of the molecule is shown in Fig. 3.

The potentially bidentate picoline-functionalized benzimidazolin-2-ylidene ligand should be capable of forming a square planar platinum carbene complex like **3**. However, reaction of the 1-methyl-benzimidazolin-2-ylidene with Ag(I) and Au(I) leads to a linear structure. The coordination geometry around Pt(II) is close to square planar through the C, N, Cl-binding motif. It is believed that the –CH_2– group releases some strain in the molecule resulting in an almost square-planar geometry. The selected bond parameters are listed in Table 3.

The Pt–$C_{carbene}$ bond length [1.958(6) Å] in **3** is shorter than reported Pt-NHC complexes [1.972(8)–1.978(9) Å][58] and Pt[$(ppy)_2$]Cl system [1.973(9)–1.988(8) Å].[59,60] On the other hand, Pt–N_{py} bond length 2.039(5) Å in **3** is comparable with the Pt–N_{py} distances [1.968(5)Å] observed in Pt-CNC pincer NHC complexes of 2,6-bis(1-methylimidazoliumpyridine)-chloride ligands that has been reported recently.[63] C_{carb}–Pt (1)–Cl (1) angle 177.44(16)°, N_{py}–Pt–Cl (2) angle 176.33(14)° and other chelate angles vary from 86.9(2)–92.17(17) around Pt(II) and support its square planar geometry.

Table 1 Crystallographic parameters of **1** and **3**

	1	**3**
Empirical formula	C_{14} H_{13} N_3 Au Cl	C_{14} H_{13} Cl_2 N_3 Pt
Formula weight	455.69	489.25
Crystal system	Triclinic	Monoclinic
Space group	$P\bar{1}$	*Cc*
Temperature/K	150(2)	293
Cell dimensions		
a/Å	7.5072(14)	15.6488
b/Å	9.1676(17)	13.2247
c/Å	10.705(2)	7.1603
α (°)	79.845(4)	90
β (°)	84.056(4)	99.624
γ (°)	72.958(3)	90
Volume/Å^3	692.3(2)	1460.97
Z	2	4
Density/Mg m^{-3}	2.186	2.224
Absorption coefficient (μ)	10.806	10.0
Theta range	1.5–25	2.0–31.9
Index ranges	$-8 \le h \le 8; -10 \le k \le 10; -12 \le l \le 12$	$-19 \le h \le 19; -19 \le k \le 18; 9 \le l \le 10$
Reflections collected	6197	3667
Independent reflections	2410	0.037
Observed data/restraints/parameters	2322/0.055/173	3155/0.0370/182
GOF	1.139	0.884
Final *R* indices [$I > 2\sigma(I)$]	R_1 = 0.0356, wR_2 = 0.0966	R_1 = 0.0531, wR_2 = 0.0502
R indices (all data)	R_1 = 0.0371, wR_2 = 0.0976	R_1 = 0.0371, wR_2 = 0.0540

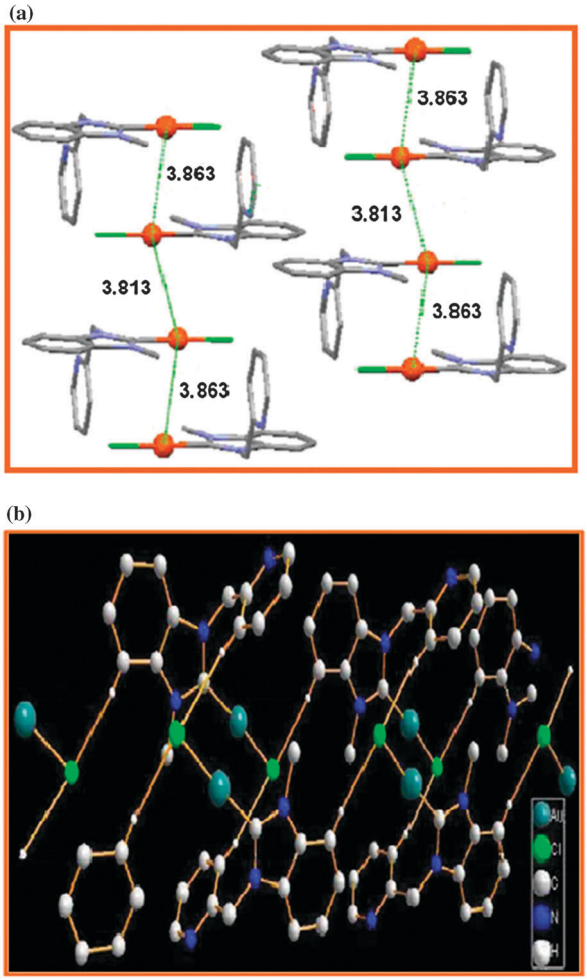

Fig. 2 (a) Au···Au interaction and (b) ID polymer through H-bonding (C–H···Cl) of complex **1**.

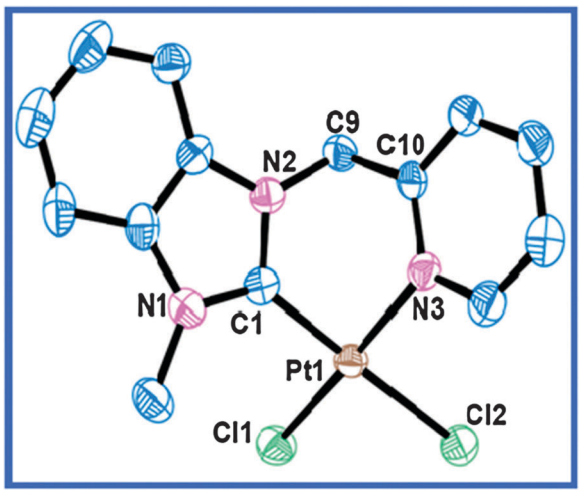

Fig. 3 ORTEP view of single crystal X-ray structure of complex **3** (50% probability, H atoms are removed for clarity).

Theoretical studies

Calculations on the electronic ground states of Pt complexes of **L1** and **L2** were carried out using the B3LYP density functional theory (DFT). LANL2DZ[52] and 6–31 G(d) basis sets were employed for Pt and Au atoms respectively. For the calculated ground-state geometries, the electronic structures were examined in terms of the highest occupied molecular orbitals (HOMOs) and the lowest unoccupied molecular orbitals (LUMOs). The molecular orbital energy calculations show that the HOMO (E_0 = −0.21368 au) is electronically more populated by benzimidazole and Pt; whereas the LUMO (E_0 = −0.08670 au) and higher LUMOs *i.e.* LUMO + 1, LUMO + 2 *etc.* are more populated by pyridine as shown in Fig. 4. Therefore, it is assumed that the charge transfer

Table 3 Selected bond lengths (Å) and bond angles (°) of **3**

Bond lengths (Å)	Bond angles (°)
Pt(1)–C(1) = 1.9(6)	C(1)–Pt(1)–Cl(2) = 108.5(7)
Pt(1)–N3 = 2.0(5)	N(3)–Pt(1)–Cl(1) = 176.1(2)
Pt(1)–Cl(1) = 2.2(16)	C(1)–Pt(1)–Cl(1) = 92.1(17)
Pt(1)–Cl(2) = 2.3(16)	C(1)–Pt(1)–N(3) = 86.9(2)
C(1)–N(1) = 1.3(7)	N(3)–Pt(1)–Cl(2) = 91.1(14)
C(1)–N(2) = 1.3(8)	Cl(1)–Pt(1)–Cl(2) = 89.9(6)
	N(1)–C(1)–N(2) = 107.9(5)

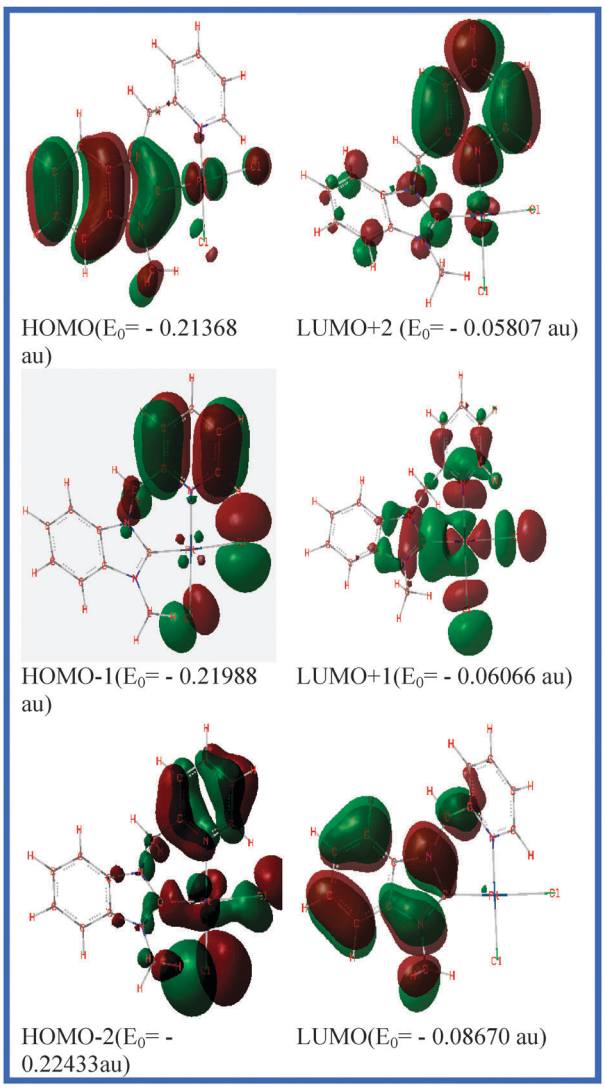

Fig. 4 Frontier MOs of complex **3**.

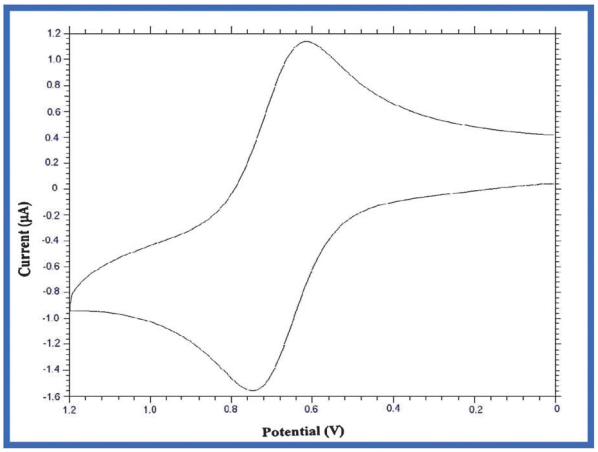

Fig. 5 Cyclic voltammogram of **3** in dry acetonitrile at 50 mV s^{-1} scan rate.

from HOMO to LUMO is mixed ILCT (interligand charge transfer)/MLCT (metal to ligand charge transfer) as described earlier.

Electrochemical studies

The cyclic voltammetric studies were carried out using a platinum electrode as working electrode in dry acetonitrile under an argon atmosphere at 50 mV s^{-1} scan rate. The cyclic voltammetric behaviors revealed the bielectronic reversible oxidation of the Pt(II)/Pt(IV) couple at 0.69 for complex **3** (shown in Fig. 5) and 0.67 eV for **4** similar to the reported Pt-*N*-heterocyclic carbene system.[64]

The lower oxidation potentials are expected because of strong σ-donor and weak π-acceptor properties of the *N*-heterocyclic carbene ligand in the Pt-*N*-heterocyclic carbene complex. The electrode potentials of **3** and **4** are also lower than that of the CN donor phenylpyridine system,[59,60] which indicates the comparatively less π-acidity of the present ligands.

Anti-proliferative activity

Out of four Au(I) and Pt(II) complexes we succeeded to study *N*-methyl substituted compounds **1** and **3** for cytotoxicity studies. The solubility of benzyl functionalized gold(I) and platinum(II) complexes **2** and **4** in culture media is very poor which keeps us away for the same study. As the benzyl group is more hydrophobic than the methyl group that may be the reason for low solubility. Antiproliferative effect of the compounds with varying concentrations (0–100 μM) was examined on B16F10 (mouse melanoma), HepG2 (human hepatocarcinoma) and HeLa (human cervical carcinoma) cell lines. The compounds show different degrees of cytotoxicity on tested cell lines. Fig. 6 shows the level of cell viability (change of optical density, O.D.) of the compounds on the three different cell lines of different origin.

The gold(I) complex, **1**, shows higher cytotoxic effect than the platinum(II) complex, **3**, on almost all the three cell lines tested. IC_{50} values of the compounds **1** and **3** and cisplatin (a platinum complex anticancer drug) on these cell lines are presented in Table 4.

IC_{50} (μM) values of **1** were found to be nearly thrice higher than cisplatin. 100 μM of **1** was treated on normal human

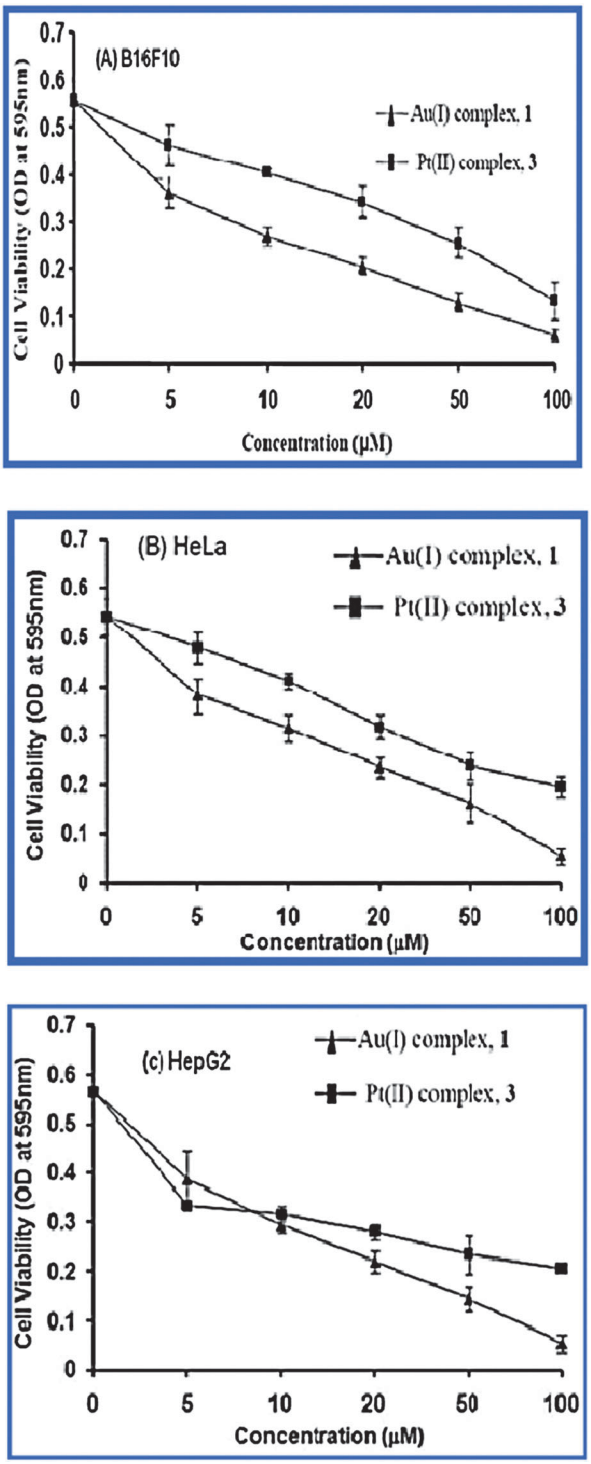

Fig. 6 Cell viability assay: 2×10^5 cells were treated with varying concentrations [0–100 μM] of complexes **1** and **3** for 24 h and an MTT assay was performed. O.D. at 595 nm presents the viability of (a) B16F10 (b) HeLa and (c) HepG2 cells. Results are from one of the three representative experiments. Values are mean ± S.D.

peripheral blood mono nuclear cells and it did not show any significant cytotoxic effect (data not shown), whereas 10 μM of cisplatin showed 75 ± 4.5% cytotoxicity on normal human peripheral mononuclear blood cells. Apparently, potency of compound **1** was found to be relatively low to cisplatin and

Table 4 IC_{50} (μM) values of different cancer cell lines

	B16F10	HeLa	HepG2
Au(I)-compound, **1**	33.79 ± 0.94	26.97 ± 2.4	29.48 ± 3.4
Pt(II)-compound, **3**	62.41 ± 3.0	52.675 ± 5.3	48.43 ± 5.1
Cisplatin	7.4 ± 1.66	6.5 ± 1.7	6.5 ± 1.7

Au(I)-NHC complexes reported by Gautier's group.[30] Compounds which are capable of inducing cell death *via* apoptosis are regarded as potent anticancer drugs. Cell shrinkage and rounding, membrane blebbing, chromatin condensation and nuclear fragmentation are important characteristics of apoptosis. 4′-6-Diamidino-2-phenylindole (DAPI) is a nuclear staining dye that intercalates within the base pairs and fluoresces when it is excited with UV light. Any nuclear change can be visualized by using DAPI. In our study, prominent morphological changes, which are associated with apoptosis, like cell rounding and shrinkage and nuclear fragmentation, were observed when B16F10, HepG2 and HeLa cells were treated with the more potent complex **1** (25 μM) for 24 h (Fig. 7).

Conclusion

This article presents a survey of synthesis, structures, and electrochemistry of the metal-*N*-heterocyclic carbenes of Au(I) and Pt(II) complexes (**1–4**). Novel gold(I) and platinum(II) complexes were synthesized and well characterized in detail by NMR and X-ray analysis. The Pt(II) is in a square-planar coordination environment with the ligand having a bidentate (C,N) chelating motif, whereas Au(I) adopts the bi-coordinated linear geometry. Both the compounds **1** and **3** show modest *in vitro* cytotoxic properties against various cancer cell lines, *e.g.* B16F10 (mouse melanoma), HepG2 (human hepatocarcinoma) and HeLa (human cervical carcinoma). IC_{50} values are compared with cisplatin and the results revealed that complex **1** possesses better activity than **3**. More detailed studies are needed to understand the mechanisms of action at the cellular level and the role of the metals.

Experimental section

General procedures

All the reagents 1-methylbenzimidazole, Ag_2O, K_2PtCl_4, 2-poicolylchloride hydrochloride were purchased from Sigma-Aldrich, UK, and were used without further purification. $Au(SMe_2)Cl$ was prepared according to the literature[48]. All manipulations were carried out under an open atmosphere unless otherwise stated. All the solvents were distilled over appropriate dry agents and N_2-saturated prior to use. Electronic spectra of the complexes were obtained on a Shimadzu UV-1601. ^1H and ^{13}C NMR spectra were recorded on

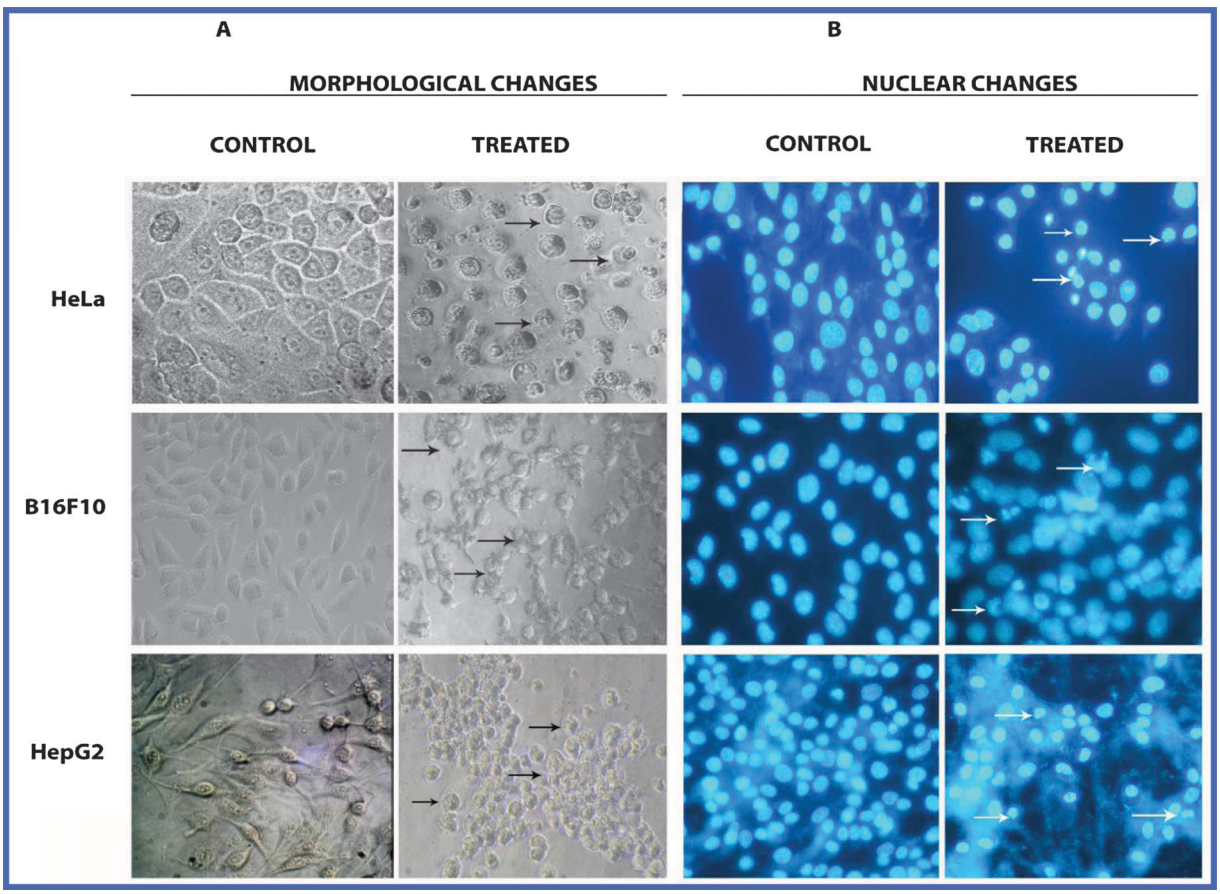

Fig. 7 Cells treated with or without 25 μM of **1** for 24 h. Morphological changes: DAPI staining also revealed bluish intact nuclei in control cells along with nuclear condensation, nuclear blebbing and nuclear fragmentation on the treated cells. These characteristic changes indicate that complex **1** induced cell death is mostly *via* apoptosis (shown by arrows).

Bruker 400 and 300 MHz spectrometers. Chemical shifts, δ, are reported in ppm relative to the internal standard TMS for both ^{1}H and ^{13}C NMR. J values are given in Hz. Elemental analyses are performed using a Perkin–Elmer 2400 C elemental analyzer. The cyclic voltammetric studies were carried out in a CH 600 analyzer using a platinum electrode as working electrode.

General syntheses

Synthesis of 1-methyl-3-(2-pyridylmethyl)-1*H* benzimidazolium-chloride, L1. Synthesis of the bromide salt of the proligand is reported earlier.[49] *We have synthesized chloride salt of the same* with slight modification; 1-methylbenzimidazole (500 mg, 3.79 mmol) and 2-picolylchloride hydrochloride (621 mg, 3.79 mmol) and $NaHCO_3$ (414 mg, 4.93 mmol) were taken in EtOH and refluxed for 24 h. Then the solvent was removed and the gummy mass was suspended in dichloromethane, then filtered; to the clear tea red solution cold Et_2O was added and the ppt was filtered to get a moisture sensitive solid mass. Yield was 855.6 mg, 3.29 mmol, 87%. ^{1}H NMR (400 MHz, CD_3CN): δ = 9.10 (s, 1 H, N*CH*N), 8.53 (d, J = 5.2 Hz, 1H, pyridine-H), 7.90–7.82 (m, 3H, Ar-H), 7.75–7.66 (m, 2H, pyridine-H and pyridine-H), 7.56 (d, J = 4.8 Hz, 1H, pyridine-H), 7.39–7.36 (m, 1H, Ar-H), 5.77 (s, 2H, NCH_2-pyridine), 4.10 (s, 3H, NCH_3) ppm. ^{13}C NMR (400 MHz, CD_3CN): δ = 152.1, 149.6, 141.8, 137.3, 131.8, 131.2, 126.8, 126.7, 123.6, 122.5, 113.3, 113.1, 51.2, 33.1 ppm. Anal. calcd for $C_{14}H_{14}N_3Cl$: C, 64.74; H, 5.395; N, 16.185%. Found: 64.45; H, 4.89; N, 15.79%.

Synthesis of 1-benzyl-3-(2-pyridylmethyl)-1*H* benzimidazolium-chloride, L2. 1-Benzylbenzimidazole (500 mg, 2.4 mmol) and 2-picolylchloride hydrochloride (316 mg, 1.93 mmol) and $NaHCO_3$ (211 mg, 2.51 mmol) were taken in EtOH and refluxed for 28 h, rest of the procedure has been repeated as for **L1**. Yield was 564 mg, 1.68 mmol, 70%. The synthesis of the proligand **L2** is reported earlier.[50]

1-Methyl-3-(2-pyridylmethyl)benzimidazolinegold(I)chloride, 1. Silver oxide (600 mg, 2.59 mmol) and 1-methyl-3-(2-pyridyl-methyl)-1*H* benzimidazoliumchloride, **L1** (337.4 mg, 1.30 mmol), were taken in dry dichloromethane and the solution was stirred for 4 h in dark, then the solution was filtered through celite to remove excess Ag_2O. Into the clear filtrate, $Au(SMe_2)Cl$ (383 mg, 1.30 mmol) was added dropwise and immediate white ppt was observed, the mixture was stirred for 1.5 h and filtered through celite. The solvent was removed and the white mass was recrystallized from dichloromethane and diethyl ether. Yield was 414 mg (0.91 mmol, 70%). ^{1}H NMR (400 MHz, CD_3CN): δ = 8.62 (d, J = 5.2 Hz, 1H, pyridine-H), 8.19 (t, J = 7.8 Hz, 2H, Ar-H), 7.85 (d, J = 8.2 Hz, 1H, Ar-H), 7.69 (d, J = 8.1, 1H, -pyridine-H), 7.78 (d, J = 8.2 Hz, H, Ar-H), 7.69 (d, J = 8.0, 1H, -pyridine-H), 7.57 (t, J = 7.8 Hz, 1H, -pyridine-H), 6.12 (d, J = 14.0 Hz, 2 H, NCH_2-pyridine), 4.08 (s, 3H, NCH_3) ppm. ^{13}C NMR (400 MHz, CD_3CN): δ = 168.4, 155.5, 152.2, 141.8, 134.0, 132.6, 125.5, 125.1, 124.5, 124.2, 112.0, 111.5, 55.4, 34.6 ppm. Anal. calcd for $AuC_{14}H_{13}N_3Cl$: C, 36.88; H, 2.85; N, 9.22%. Found: 36.65; H, 2.93; N, 9.14%.

1-Benzyl-3-(2-pyridylmethyl)-benzimidazolinegold(I)chloride, 2. Silver oxide (600 mg, 2.59 mmol) and 1-benzyl-3-(2-pyridyl-methyl)-1*H* benzimidazoliumchloride **L2** (435 mg, 1.30 mmol) were taken in dry dichloromethane and the solution was stirred for 4 h in dark, then the solution was filtered through celite to remove excess Ag_2O. Into the clear filtrate $Au(SMe_2)Cl$ (382 mm, 1.30 mmol) was added and immediate white ppt was observed, the mixture was stirred for 1.5 h and filtered through celite. The solvent was removed and the white mass was recrystallized from dichloromethane and diethyl ether. Yield was 469 mg (0.88 mmol, 68%). ^{1}H NMR (400 MHz, DMSO-d_6): d 8.54 (d, J = 4.4 Hz, pyridine, 1H), 7.92 (m, 1H), 7.76 (m, 1H), 7.71 (m, 2H), 7.40–7.38 (m, 2H),7.33–7.27 (m, 3H), 5.98 (s, CH_2, 2H), 5.78 (s, CH_2, 2H). ^{13}C NMR (400 MHz, DMSO-d_6): δ 168.5, 155.7, 153.4, 149.9, 137.7, 136.7, 134.3, 133.7,129.2, 129.1, 128.4, 127.7, 124.7, 122.7, 112.8, 55.7, 53.3. Anal. calcd for $C_{20}H_{17}N_3AuCl$: C, 45.16; H, 3.20; N, 7.90%. Found: C, 44.64; H, 3.08; N, 7.64%.

1-Methyl-3-(2-pyridylmethyl)-benzimidazolylideneplatinum(II)-chloride, 3. 1-Methyl-3-(2-pyridylmethyl)-1*H* benzimidazolium-chloride, **L1** (600 mg, 2.31 mmol), and sodium acetate (189.4 mg, 2.31 mmol) were taken in 10 ml acetonitrile and stirred for 3 h; K_2PtCl_4 (959 mg, 2.31 mmol) was added to the same mixture and stirring was continued for another 2 days. Finally, the mixture was filtered through a pack of celite; solvent was removed. The white mass was washed with water and dried over silica; the compound was recrystallized from acetonitrile and diethyl ether. Yield was 621.2 mg (1.27 mmol, 55%). ^{1}H NMR (400 MHz, CD_3CN): δ = 8.84 (d, J = 5.4 Hz, 1H, pyridine-H), 8.25 (t, J = 7.8 Hz, 1H, pyridine-H), 7.91 (d, J = 7.6 Hz, 1H, Ar-H and pyridine-H), 7.82 (d, J = 7.8 Hz, 2H, Ar-H), 7.57–7.51 (m, 2H, Ar-H), 7.48 (m, H, pyridine-H), 6.14 (d, J = 14.6 Hz, 2H, NCH_2-pyridine), 4.10 (s, 3H, NCH_3) ppm. ^{13}C NMR (400 MHz, CD_3CN): δ = 184.5, 157.4, 153.8, 143.6, 136.5, 133.2, 126.4, 125.4, 125.2, 125.5, 112.2, 111.6, 56.3, 34.8 ppm. Anal. calcd for $PtC_{14}H_{13}N_3Cl_2$: C, 34.35; H, 2.66; N, 8.59%. Found: 33.15; H, 2.76; N, 8.05%.

1-Benzyl-3-(2-pyridylmethyl)-benzimidazolylideneplatinum(II)-chloride, 4. Compound **4** was prepared similar to **3**; **L2** (600 mg, 1.79 mmol), sodium acetate (147 mg, 1.79 mmol) and K_2PtCl_4 (743 mg, 1.79 mmol) were taken in acetonitrile and rest of the method is the same as that reported earlier. Yield was 525 mg (0.93 mmol), 52%).^{1}H NMR (400 MHz, DMSO-d_6): δ 8.83 (d, J = 5.2 Hz, 1H, pyridine-H), 8.26 (t, J = 7.8 Hz, 1H, pyridine-H), 7.93–7.91 (m, 1H, pyridine-H), 7.91 (d, J = 7.8 Hz, 2H, Ar-H), 7.76 (t, J = 7.8 Hz, 2H, Ar-H), 7.71–7.68 (m, 2H, Ar-H), 7.65 (t, J = 7.6 Hz, 1H, Ar-H), 7.33–7.27 (m, 2H, Ar-H), 6.12 (d, J = 14.6 Hz, 2H, NCH_2-pyridine), 5.98 (s, 2H, NCH_2-Ar). ^{13}C NMR (400 MHz, CD_3CN): δ = 184.2, 157.1, 153.6, 143.7, 136.5, 133.2, 126.4, 126.2, 125.5, 125.3, 125.0, 124.8, 112.5, 111.2, 111.1, 56.3, 54.4. Anal. calcd for $PtC_{20}H_{17}N_3Cl_2$: C, 42.48; H, 3.01; N, 7.43%. Found: 41.44; H, 3.13; N, 7.45%.

Crystal structures determination

Single crystals suitable for data collection were grown from slow diffusion of diethyl ether into a saturated dichloromethane solution in the case of **1**; whereas slow diffusion of diethyl ether

into a saturated acetonitrile solution of **3** leads to block shaped colourless crystals. The crystal data and details of the data collections for **1** and **3** are given in Table 1. X-Ray data were collected on a CCD diffractometer (graphite monochromated MoKα radiation, λ = 0.71073 Å) by use of ω scans. The structures were solved by direct methods and refined on F2 using all reflections with SHELX-97.[51] The nonhydrogen atoms were refined anisotropically. Hydrogen atoms, which were not bound to imidazolium-C2 atoms, were placed in calculated positions and assigned to an isotropic displacement parameter of 0.08 Å. CCDC No. 834096 and 834097 for compound **1** and **3**, respectively, contain the supplementary crystallographic data for this paper.

Theoretical studies

Geometries of Au(I) and Pt(II) complexes were optimized at the B3LYP/LANL2DZ level of theory using the Gaussian 03W[52] program. The number of imaginary frequencies of all the molecules turns out to be zero, implying that they correspond to minimum energy structures on the potential energy surface. The frontier molecular orbitals of these complexes were generated in Gaussview using the same level of theory.

Electrochemical studies

Cyclic voltammetry was studied under an argon atmosphere on a CH 600 analyzer using a platinum electrode as working electrode, Ag/AgCl as reference electrode, tetrabutylammonium hexaflurophosphate (0.1 M) as supporting electrolyte and dry acetonitrile as solvent.

Antiproliferative assay *in vitro*

The anti-proliferative tests were performed on mouse and human cancer lines B16F10 (mouse melanoma), HepG2 (human hepatocarcinoma) and HeLa (human cervical carcinoma). Twenty four hours before addition of the tested compounds, the cell lines were plated in 96-well plates (Sarstedt, Germany) at a density of 10^4 cells per well and were cultured in the mixture medium. An MTT [3-(4, 5-dimethylthiazol-2-yl)-2,5-diphenyltetrazolium bromide] assay was used to evaluate cell viability as previously described.[53] Briefly, cells were seeded into 96-well culture plates in triplicate. Monolayers of cells were treated with compounds **1** or **3** at concentrations ranging from 0–100 µM for 0–24 h. At the end of the culture period, 20 µl of 5 mg ml^{-1} MTT stock solution was added into each well. After additional 4 h incubation at 37 °C, the resultant intracellular formazan crystals were solubilized with acidic isopropanol and the absorbance of the solution was measured at 595 nm using an ELISA reader (Model: Emax, Molecular device, USA). The *in vitro* cytotoxic effect of all compounds was examined after 24 h exposure of the cultured cells to varied concentrations of the tested compounds, using the 3-(4,5-dimethylthiazol-2-yl)-2,5 diphenyltetrazolium bromide assay for adherent cells. The results are presented as an IC_{50} (inhibitory concentration 50%) concentration (µg ml^{-1} of tested agent, which inhibits proliferation of 50% of cancer cells population). IC_{50} values are calculated separately for each experiment. Each compound was tested at every concentration in triplicate in a single experiment, which was repeated 3 times.

Microscopic study

To detect cellular death, treated and untreated cells were washed twice with PBS and viewed under a light microscope. Morphological changes were observed. To detect nuclear damage or chromatin condensation, cells were fixed with 3.7% *para*-formaldehyde at room temperature for 2 h. Fixed cells were stained with 10 µg ml^{-1} of 4′,6′-diamidino-2-phenylindole (DAPI) and observed under a fluorescence microscope (Model: OLYMPUS IX70, Olympus Optical Co. Ltd., Shibuya-ku, Tokyo, Japan) with excitation at 359 nm and emission at 461 nm[54] and images were acquired.

Acknowledgements

JD thanks Department of Science and Technology, DST, India, for financial support under SERC Fast Track Young Scientist Scheme (SR/FT/CS-046/2009) and Prof. N. Bhattacharya, HIT for constant encouragement.

References

1 D. Bourissou, O. Guerret, F. P. Gabbai and G. Bertrand, *Chem. Rev.*, 2000, **100**, 39–92.
2 P. de Fremont, N. Marion and S. P. Nolan, *Coord. Chem. Rev.*, 2009, **253**, 862–892.
3 Y. Canac, M. Soleilhavoup, S. Conejero and G. J. Bertrand, *J. Organomet. Chem.*, 2004, **689**, 3857–3865.
4 M. Melaimi, M. Soleilhavoup and G. Bertrand, *Angew. Chem., Int. Ed.*, 2010, **49**, 8810–8849.
5 O. Schuster, L. Yang, H. G. Raubenheimer and M. Albrecht, *Chem. Rev.*, 2009, **109**, 3445–3478.
6 K. Ofele, E. Tosch, C. Taubmann and W. A. Herrmann, *Chem. Rev.*, 2009, **109**, 3408–3444.
7 H.-W. Wanzlick, *Angew. Chem., Int. Ed. Engl.*, 1962, **1**, 75–80.
8 H.-W. Wanzlick and H. J. Scheonherr, *Angew. Chem., Int. Ed. Engl.*, 1968, **7**, 141–142.
9 A. J. Arduengo III, R. L. Harlow and M. A. Kline, *J. Am. Chem. Soc.*, 1991, **113**, 361–363.
10 W. A. Hermann and C. Kocher, *Angew. Chem., Int. Ed. Engl.*, 1997, **36**, 2162–2187.
11 W. A. Hermann, *Angew. Chem., Int. Ed.*, 2002, **41**, 1290–1309.
12 F. E. Hahn and M. C. Jahnke, *Angew. Chem.*, 2008, **120**, 3166–3179.
13 Recent developments in the organometallic chemistry of *N*-heterocyclic carbenes (ed. R. H. Crabtree), 2007.
14 N. Marion, S. Díez-González and S. P. Nolan, *Angew. Chem.*, 2007, **119**, 3046–3050 (*Angew. Chem., Int. Ed.*, 2007, **46**, 2988–3000).
15 A. J. Arduengo, III, *Acc. Chem. Res.*, 1999, **32**, 913–921.
16 W. A. Herrmann and C. Kochner, *Angew. Chem., Int. Ed.*, 1997, **36**, 2163–2187.
17 E. Peris and R. H. Crabtree, *Coord. Chem. Rev.*, 2004, **248**, 2239–2246.
18 C. M. Crudden and D. P. Allan, *Coord. Chem. Rev.*, 2004, **248**, 2247–2273.
19 D. Puch and A. A. Danopoulos, *Coord. Chem. Rev.*, 2007, **251**, 610–641, and ref. therein.
20 F. Guillen, C. L. Winn and A. Alexakis, *Tetrahedron: Asymmetry*, 2001, **12**, 2083–2208.
21 R. H. Crabtree, *J. Organomet. Chem.*, 2005, **690**, 5451–5457.
22 E. Peris, J. Mata, J. A. Loch and R. H. Crabtree, *Chem. Commun.*, 2001, 201–202.
23 (*a*) J. R. Miecznikowski, S. Gruendemann, M. Albrecht, C. Megret, E. Clot, J. W. Faller, O. Eisenstein and R. H. Crabtree, *Dalton Trans.*, 2003, 831–838; (*b*) A. G. Tennyson, V. M. Lynch and C. W. Bielawski, *J. Am. Chem. Soc.*, 2010, **132**, 9420–9429; (*c*) T. W. Hudnall, A. G. Tennyson and C. W. Bielawski, *Organometallics*, 2010, **29**, 4569–4578; (*d*) D. M. Khramov, E. L. Rosen, J. A. V. Er, P. D. Vu, V. M. Lynch and C. W. Bielawski, *Tetrahedron*, 2008, **64**, 6853–6862.

24 B. Wang, D. Wang, D. Cui, W. Gao, T. Tang, X. Chen and X. Jing, *Organometallics*, 2007, **26**, 3167–3172.
25 B. Rosenberg, L. Vancamp, J. E. Trosko and V. H. Mansour, *Nature*, 1969, **222**, 385–386.
26 G. Jaouen and A. Vessières, *Pure Appl. Chem.*, 1985, **57**, 1865–1874.
27 P. J. Dyson, *Chimia*, 2007, **61**, 698–703.
28 S. J. Dougan and P. J. Sadler, *Chimia*, 2007, **61**, 704–715.
29 L. D. Dale, J. H. Tocher, T. M. Dyson, D. I. Edwards and D. A. Tocher, *Anti-Cancer Drug Des.*, 1992, **7**, 3–14.
30 M.-L. Teyssot, A.-S. Jarrousse, M. Manin, A. Chevry, S. Roche, F. Norre, C. Beaudoin, L. Morel, D. Boyer, R. Mahiou and A. Gautier, *Dalton Trans.*, 2009, 6894–6902.
31 X.-M. Zhu, X.-Y. Zhang, X.-J. Liu, G.-F. Liu Wang, A. Usman and H.-K. Fun, *Inorg. Chem. Commun.*, 2003, **6**, 1113–1116.
32 B. Thati, A. Noble, B. S. Creaven, M. Walsh, M. McCann, K. Kavanagh, M. Devereux and D. A. Egan, *Cancer Lett.*, 2007, **248**, 321–333.
33 J. J. Liu, P. Galettis, A. Farr, L. Maharaj, H. Samarasinh, A. C. McGechan, B. C. Baguley, R. J. Bowen, S. J. B. Price and M. J. McKeage, *J. Inorg. Biochem.*, 2008, **102**, 303–310.
34 P. J. Barnard, M. V. Baker, S. J. B. Price and D. A. Day, *J. Inorg. Biochem.*, 2004, **98**, 1642–1647.
35 M. V. Baker, P. J. Barnard, S. J. B. Price, S. K. Brayshaw, J. L. Hickey, B. W. Skelton and A. H. White, *Dalton Trans.*, 2006, 3708–3715.
36 M. V. Baker, P. J. Barnard, S. J. B. Price, S. K. Brayshaw, J. L. Hickey, B. W. Skelton and A. H. White, *J. Organomet. Chem.*, 2005, **690**, 5625–5635.
37 J. L. Hickey, R. A. Ruhayel, P. J. Barnard, M. V. Baker, S. J. B. Price and A. Filipovska, *J. Am. Chem. Soc.*, 2008, **130**, 12570–12571.
38 S. Ray, R. Mohan, J. K. Singh, M. K. Samantaray, M. M. Shaikh, D. Panda and P. Ghosh, *J. Am. Chem. Soc.*, 2007, **129**, 15042–15053.
39 P. Baxter, J.-M. Lehn, A. DeCian and J. Fischer, *Angew. Chem., Int. Ed. Engl.*, 1993, **32**, 69–72.
40 S. Leininger, B. Olenyuk and P. J. Stang, *Chem. Rev.*, 2000, **100**, 853–907.
41 F. A. Cotton, C. Lin and C. A. Murillo, *Acc. Chem. Res.*, 2001, **34**, 759–771.
42 A. M. Pizarro and P. J. Sadler, in *Nucleic Acid-Metal Ion Interactions*, ed. N. V. Hud, Royal Society of Chemistry, Cambridge, 2009, ch. 10, p. 358.
43 E. R. T. Tiekink, *Inflammopharmacology*, 2008, **16**, 138–142; I. Ott, *Coord. Chem. Rev.*, 2009, **253**, 1670–1681; and references cited herein.
44 M. V. Baker, P. J. Barnard, S. J. Berners-Price, S. K. Brayshaw, J. L. Hickey, B. W. Skelton and A. H. White, *J. Organomet. Chem.*, 2005, **690**, 5625–5635.
45 P. de Fremont, E. D. Stevens, M. D. Eelman, D. E. Fogg and S. P. Nolan, *Organometallics*, 2006, **25**, 5824–5828.
46 P. J. Barnard and S. J. Berners-Price, *Coord. Chem. Rev.*, 2007, **251**, 1889–1902.
47 J. L. Hickey, R. A. Ruhayel, P. J. Barnard, M. V. Baker, S. J. Berners-Price and A. Filipovska, *J. Am. Chem. Soc.*, 2008, **130**, 12570–12571.
48 R. Uson, A. Laguna and M. Laguna, *Inorg. Synth.*, 1989, **26**, 85–91.
49 M. C. Jahnke, T. Pape and F. E. Hahn, *Eur. J. Inorg. Chem.*, 2009, 1960–1969.
50 (*a*) X. Zhang, S. Gu, Q. Xia and W. Chen, *J. Organomet. Chem.*, 2009, **694**, 2359–2367; (*b*) A. G. Tennyson, E. L. Rosen, M. S. Collins, V. M. Lynch and C. W. Bielawski, *Inorg. Chem.*, 2009, **48**, 6924–6933; (*c*) A. J. Boydston, J. D. Rice, M. D. Sanderson, O. L. Dykhno and C. W. Bielawski, *Organometallics*, 2006, **25**, 6087–6098.
51 G. M. Sheldrick, *SHELX-97, Program for Crystal Structure Refinement*, University of Gottingen, Germany, 1997.
52 M. J. Frisch, G. W. Trucks, H. B. Schlegel, G. E. Scuseria, M. A. Robb, J. R. Cheeseman, J.A. Montgomery Jr., T. Vreven, K. N. Kudin, J. C. Burant, J. M. Millam, S. S. Iyengar, J. Tomasi, V. Barone, B. Mennucci, M. Cossi, G. Scalmani, N Rega, G. A. Petersson, H. Nakatsuji, M. Hada, M. Ehara, K. Toyota, R. Fukuda, J. Hasegawa, M. Ishida, T. Nakajima, Y. Honda, O. Kitao, H. Nakai, M. Klene, X. Li, J. E. Knox, H. P. Hratchian, J. B. Cross, V. Bakken, C. Adamo, J. Jaramillo, R. Gomperts, R. E. Stratmann, O. Yazyev, A. J. Austin, R. Cammi, C. Pomelli, J. Ochterski, P. Y. Ayala, K. Morokuma, G. A. Voth, P. Salvador, J. J. Dannenberg, V. G. Zakrzewski, S. Dapprich, A. D. Daniels, M. C. Strain, O. Farkas, D. K. Malick, A. D. Rabuck, K. Raghavachari, J. B. Foresman, J. V. Ortiz, Q. Cui, A. G. Baboul, S. Clifford, J. Cioslowski, B. B. Stefanov, G. Liu, A. Liashenko, P. Piskorz, I. Komaromi, R. L. Martin, D. J. Fox, T. Keith, M. A. Al-Laham, C. Y. Peng, A. Nanayakkara, M. Challacombe, P. M. W. Gill, B. G. Johnson, W. Chen, M. W. Wong, C. Gonzalez and J. A. Pople, *Gaussian 03, Revision B.03*, Gaussian, Inc., Pittsburgh, PA.
53 T. Mossman, Rapid colorimetric assay for cellular growth and survival, *J. Immunol.Methods*, 1983, **65**, 55–63.
54 J. J. Cohen, Apoptosis, *Immunol. Today*, 1993, **14**, 126–130.
55 H. M. Wang and I. J. B. Lin, *Organometallics*, 1998, **17**, 972–975.
56 J. C. Garrison and W. J. Youngs, *Chem. Rev.*, 2005, **105**, 3978–4008 and ref. therein.
57 J. C. Y. Lin, R. T. W. Huang, C. S. Lee, A. Bhattacharyya, W. S. Hwang and I. J. B. Lin, *Chem. Rev.*, 2009, **109**, 3561–3598.
58 S. Fantasia, J. L. Petersen, H. Jacobsen, L. Cavallo and S. P. Nolan, *Organometallics*, 2007, **26**, 5880–5889.
59 T. Okada, I. M. El-Mehasseb, M. Kodaka, T. Tomohiro, K.-I. Okamoto and H. Okuno, *J. Med. Chem.*, 2001, **44**, 4661–4667.
60 J.-C. Shi, H.-Y. Chao, W.-F. Fu, S.-M. Peng and C.-M. Che, *J. Chem. Soc., Dalton Trans.*, 2000, 3128–3132.
61 V. J. Catalano and A. L. Moore, *Inorg. Chem.*, 2005, **44**, 6558–6566.
62 V. J. Catalano and A. L. Moore, *Inorg. Chem.*, 2007, **46**, 5608–5615.
63 C.-S. Lee, S. Sabiah, J.-C. Wang, W.-S. Hwang and I. J. B. Lin, *Organometallics*, 2010, **29**, 286–289.
64 S. D. Adhikary, T. Samanta, G. Roymahapatra, F. Loiseau, D. Jouvenot and J. Dinda, *New J. Chem.*, 2010, **34**, 1974–1980.